

# Capacity-time Trade-off in Highly Reliable Quantum Memory

Miao-Miao Yi,<sup>1</sup> L. X. Cui,<sup>2,3</sup> Y -M. Du,<sup>1,\*</sup> and C. P. Sun<sup>1,†</sup>

<sup>1</sup>*Graduate School of China Academy of Engineering Physics, Beijing, 100193, China*

<sup>2</sup>*Beijing Computational Science Research Center, Beijing, 100193, China*

<sup>3</sup>*International Research Center for Neurointelligence,  
University of Tokyo Institutes for Advanced Study,  
University of Tokyo, Bunkyo-ku, Tokyo, 113-0033, Japan*

Reliable optical quantum memory is limited by real-world imperfections such as disordered coupling and detuning. Existing studies mostly address these factors separately, while in practice their correlated effects set a fundamental limit on storage performance. We develop a comprehensive model that simultaneously incorporates disordered coupling and detuning. It is shown that these disorders induce a random Berry's phase in the stored states, while decoherence from disordered coupling stems from correlations with detuning rather than individual imperfections. This mechanism imposes a fundamental trade-off among storage capacity, storage time, and driving time, setting a universal limit for reliable storage. Extending the analysis to memory based devices operating with multiple storage processes shows that enhancing parameter independence improves their reliability. We further provide a more precise relation for measuring and correcting global detuning, which is directly relevant to current experimental protocols.

*Introduction.*— Quantum memory is a system that can store and retrieve a quantum state on demand, which holds significant importance for advancing numerous fields including quantum communication [1–3] and quantum computation [3–5]. A high-quality quantum storage must satisfy several essential criteria: (1) a long storage time [3, 6, 7], (2) large capacity and universality for storing arbitrary states [3, 8, 9], and (3) a perfect store-in-retrieve-out (SIRO) process without destructing information. Driven by these requirements, many theoretical schemes have been proposed, particularly those based on atomic ensembles [10–13].

In practice, faithfully implementing the ideal designs remains a technical challenge. An important difficulty arises when increasing the number of atoms to achieve high capacity, as unavoidable disorder is introduced, including disordered light-atom coupling strength [12, 14], disordered detuning induced by linewidth [15], inhomogeneous broadening [16]. Notably, the average detuning is typically nonzero due to AC-stark shift [17–19] and even intentionally introduced in certain protocols [13, 20, 21]. These disorders could potentially compromise perfect storage, and elucidating their impact and underlying mechanisms remain a key objective of current research, which is crucial for optimization the performance of quantum memory.

It is plausible that disorder in system could constrain storage capacity and time. Physically, the presence of disorders effectively renders the memory equivalent to an intrinsic reservoir, which induces decoherence of states that increases with storage time. This makes it difficult to realize both high capacity and long storage time. In fact, the influence of disorder on such essential criteria of a quantum memory, especially the capacity, has not been investigated. Furthermore, it is the common practice in previous studies to discuss the impact of disorder by con-

sidering individual factors in isolation, which even leads to many nontrivial results. For instance, while disordered coupling strength results in collective decoherence of free evolution [12], Ref.[22] reports that dark-state-based protocols (e.g., EIT and Raman) remain unaffected. Moreover, several protocols, such as those in nuclear-spin system [23–25] likewise rely on this conclusion. Indeed, the correlated effects among different realistic origins of disorders can lead to markedly different results, but they are rarely studied. Qualitatively, certain factors (e.g., detuning) can induce a random phase that contains contributions from different disorders and their cross-correlations, the latter inducing decoherence that can far exceed the individual ones.

In this letter, we establish a comprehensive model for the EIT-based protocol [9–11] to simultaneously investigate the effects of disordered coupling strength and detuning on the storage of general quantum states. Here, we classify the mean of the disordered detuning as global detuning, and its fluctuations as broadening. Within the quantum reliability framework [26–29] for assessing the performance of memory and the key operational processes in memory-based devices, such as quantum repeaters and synchronizer, it is shown that these factors primarily damage the information of the stored state by inducing a random Berry's phase. This imposes a limitation to storage capacity, and on the basis a universal trade-off among storage capacity, storage and driving time is established for a reliable memory. Furthermore, we obtain a precise phase-detuning relation, which improves the accuracy of detuning measurement and compensation, and can be directly applied in recent experimental schemes.

*Model.*—We consider the system consists of  $N$   $\Lambda$ -type three-level atoms shown in Fig. 1. For the  $j$ -th atom, the ground state, excited state and metastable state are

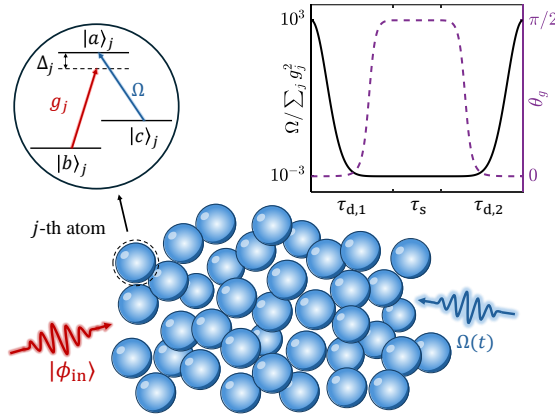


FIG. 1. Schematic of a quantum memory system composed of  $N$  three-level atoms, where atoms are coupled to a classical control field (blue) and a quantum mode (red). The upper-right panel illustrates the classical driving pulse  $\Omega(t)$  (black solid line) and the corresponding angle  $\theta_g(t)$  (purple dashed line) over three time intervals to realize a SIRO process. Here, a Gaussian pulse is taken as an example,  $\Omega/\sum_j g_j^2 = \xi \exp(-2 \ln(\xi)(t/\tau_{d,1})^2)$  for store-in, with the inverse procedure used for retrieval, here we set  $\xi = 1000$ .

labeled by  $|b\rangle_j$ ,  $|a\rangle_j$  and  $|c\rangle_j$ , respectively. The  $|b\rangle_j \rightarrow |a\rangle_j$  transition couples to a quantized mode that carries information, with coupling strength  $g_j$ , while  $|c\rangle_j \rightarrow |a\rangle_j$  couples to a classical control field with Rabi frequency  $\Omega_j$ . In the interaction picture, the Hamiltonian follows as ( $\hbar = 1$ )

$$\hat{H} = \hat{a} \sum_{j=1}^N g_j \exp(i\Delta_j t) \exp(i\mathbf{K}_{ba} \cdot \mathbf{r}_j) \hat{\sigma}_{ab}^{(j)} + \sum_j \Omega_j(t) \exp(i\delta_j t) \exp(i\mathbf{K}_{ca} \cdot \mathbf{r}_j) \hat{\sigma}_{ac}^{(j)} + \text{H.c.}, \quad (1)$$

where  $\mathbf{r}_j$  represents the position of the  $j$ -th atom,  $\mathbf{K}_{ba}(\mathbf{K}_{ca})$  is the wave vector of the quantum (classical) field,  $\hat{a}$  is the annihilation operator of quantized mode, and  $\hat{\sigma}_{\mu\nu}^{(j)} = |\mu\rangle_j \langle \nu|$  ( $\mu, \nu = a, b, c$ ) is the quasi-spin operator described for the transition  $|\nu\rangle_j \rightarrow |\mu\rangle_j$ . Here,  $\Delta_j$  ( $\delta_j$ ) represents the unavoidable detuning between quantum (classical) field and  $j$ -th atom. To simplify the discussion while capturing the essential physics, we consider  $\delta_j \equiv 0$ , and  $\Omega_j(t) \equiv \Omega(t)$ ,  $\forall j$ . Furthermore, we model each detuning and coupling strength satisfy independent normal distribution  $\Delta_j \sim \mathcal{N}(\Delta, \delta\Delta^2)$ ,  $g_j \sim \mathcal{N}(g, \delta g^2)$ ,  $\forall j$ . Physically, the mean values  $\Delta$  and  $g$  correspond to the global detuning and average coupling strength, while the variances  $\delta\Delta$  and  $\delta g$  describe the broadening [16] and disordered coupling strength [12].

We consider  $N \gg 1$  and low excitation condition [9, 20, 23], where the occupation number in the excited (metastable) state within the atomic ensemble are negli-

gible compared to  $N$ . We focus on the zero eigen-value dark-states employed in quantum memory [9–11]

$$|D_{\xi,n}\rangle = \frac{1}{\sqrt{n!}} (\hat{D}_{\xi}^{\dagger})^n |\mathbf{0}\rangle, \quad (2)$$

where the ground state of system (1) is defined by  $|\mathbf{0}\rangle = |0\rangle_L \otimes |0\rangle_A$  with  $H|\mathbf{0}\rangle = 0$ , here  $|0\rangle_L$  is the vacuum of Quantum field, and  $|0\rangle_A := \prod_j |b\rangle_j$  denotes the ground state of the atomic ensemble. The dark-state excited operator is  $\hat{D}_{\xi} := \hat{a} \cos \theta_g - \hat{C}_{\xi} \sin \theta_g$ , with relationships  $[\hat{D}_{\xi}, \hat{D}_{\xi}^{\dagger}] = 1$  and  $[\hat{H}, \hat{D}_{\xi}] = 0$ , where  $\tan \theta_g = (\sum_j g_j^2)^{1/2}/\Omega(t)$ . Here, the quasi-spin-wave collective excited operator is written as

$$\hat{C}_{\xi} = \sum_j^N \frac{g_j}{(\sum_k g_k^2)^{1/2}} \sigma_{bc}^{(j)} \exp(-i\mathbf{K}_{bc} \cdot \mathbf{r}_j - i\Delta_j t),$$

where subscript  $\xi = \{\Delta, g\}$  denotes a set of inhomogeneous detuning  $\Delta = (\Delta_1, \Delta_2, \dots, \Delta_N)$  and coupling  $g = (g_1, g_2, \dots, g_N)$ , the wave vector  $\mathbf{K}_{bc} = \mathbf{K}_{ba} - \mathbf{K}_{ca}$  is introduced to depict the second order transition  $|b\rangle \rightarrow |c\rangle$ . Here, further details can be found in Sec. I of Supplementary Material (SM) [30].

It is observed from Eq.(2) that  $|D_{\xi,n}\rangle = |n\rangle_L \otimes |0\rangle_A$  when  $\theta_g = 0$ , and  $|D_{\xi,n}\rangle = (-1)^n |0\rangle_L \otimes |n\rangle_A$  when  $\theta_g = \pi/2$ . Hence, as shown in Fig. 1, for a general optical stored state  $|\phi_{\text{in}}\rangle = \sum_n C_n |n\rangle_L$ , the ideal SIRO process can be divided into three stages as follows. Before storage ( $t = 0$ ), we require atomic ensemble stays in  $|0\rangle_A$ , and adjust  $\theta_g(0) = 0$  (i.e.,  $\Omega(0) \gg (\sum_j g_j^2)^{1/2}$ ). During time  $\tau_{d,1}$ , as the angle  $\theta_g$  (i.e., the driving field  $\Omega$ ) is adiabatically tuned to  $\pi/2$ , we can map the information into the atomic ensemble as  $|0\rangle_L \otimes \sum_n C_n (-1)^n |n\rangle_A$ . The state then undergoes a storage time  $\tau_s$ . Following this, during  $\tau_{d,2}$ , the state can be retrieved via the reversed procedure with  $\theta_g \rightarrow 0$ . Notably, in this letter, we consider the symmetric SIRO protocol  $\tau_{d,1} = \tau_{d,2} := \tau_d/2$ , and focus on the relatively long storage time with  $\tau_s \gg \tau_d$ . Moreover, to quantify the information-storage capacity of a universal quantum memory, we introduce the Lloyd-Shor-Devetak (LSD) capacity [31, 32]  $\mathcal{C} = \max_{\rho \in \mathcal{H}_d} [S(\Lambda(\rho)) - S(\mathcal{I} \otimes \Lambda(|\psi_{\rho}\rangle \langle \psi_{\rho}|))]$ , where  $S(\cdot)$  is the von Neumann entropy (e.g.,  $S(\rho) = -\text{Tr}(\rho \ln \rho)$ ),  $\mathcal{H}_d$  is the fully supported space, requiring the QM to store any state in the space  $\mathcal{H}_d$ .

*Reliability of quantum memory and devices.*—However, under these disorders, for a specific set of inhomogeneous  $\xi$ , the output state

$$|\phi_{\text{out},\xi}\rangle = \sum_n C_n \exp(i\gamma_{\xi,n}(\tau)) |n\rangle_L, \quad (3)$$

indeed acquires a Berry's phase throughout the entire SIRO process (please see Sec.II in SM [30]) with

$$\gamma_{\xi,n}(\tau) = -n \sum_j \frac{g_j^2 \Delta_j}{\sum_k g_k^2} \int_0^{\tau} dt \sin^2 \theta_g(t), \quad (4)$$

where  $\tau \equiv \tau_s + \tau_d$ . We then expand  $\gamma_{\xi,n}(\tau)$  around  $\Delta$  and  $g$  to first order

$$\gamma_{\xi,n}(\tau) \simeq \gamma_{\xi_0,n}(\tau) + \gamma_{\xi_0,n}(\tau)\tilde{\varepsilon}_\Delta + \mu_{\xi_0,n}(\tau)\tilde{\varepsilon}_g, \quad (5)$$

the subscript  $\xi_0 := \{\Delta_0, g_0\}$  denotes a set of homogeneous detuning  $\Delta_0 = (\Delta, \Delta, \dots, \Delta)$  and coupling strength  $g_0 = (g, g, \dots, g)$ . Here,  $\mu_{\xi_0,n}(\tau) := -\frac{n}{2}\Delta \int_0^\tau dt \sin^2(2\theta_{g_0})$ , and relative deviation  $\tilde{\varepsilon}_y := (\sum_j y_j/N - y)/y$ ,  $y = \Delta, g$ .

Such imperfect storage could degrade the memory's functionality. Since quantum memory is directly employed in quantum devices such as synchronizer [3, 33] and repeaters [1, 34, 35], which involve multiple storage operations, and different trajectories could mutually interfere. To assess the performance of quantum memory from a practical perspective, we introduce the framework of quantum reliability [26], which quantifies the deviation between realistic and ideal processes. Here, the reliability of two key operational procedures in such memory-based devices is mainly investigated: (1) Fig. A1 (a) shows single memory performing SIRO on a sequence of  $k$  states  $\{|\phi_{in}^{(1)}\rangle, \dots, |\phi_{in}^{(k)}\rangle\}$ , the reliability is denoted by  $\mathcal{R}_S(k)$ . (2) Fig. A1 (b) depicts state  $|\phi_{in}\rangle$  undergoing  $k$  QMs [34, 35], we denote reliability as  $\mathcal{R}_R(k)$ . The details and specific forms of  $\mathcal{R}_S(k)$  and  $\mathcal{R}_R(k)$  are given by Eqs.(A1), (A2) in *Appendix A*.

As illustrated by the example in Fig. A1 of *Appendix A*, the reliability loss of procedure (1) increases significantly with  $k$  compared to procedure (2), despite both involving  $k$  SIRO processes. It is noteworthy that the extra loss arises from the correlations among the collective coupling  $\mathcal{G} = \sum_j g_j$  and collective detuning  $\mathcal{D} = \sum_j \Delta_j$  across different SIRO processes. To clarify in detail, we extend to a generic  $k$ -step SIRO processes, hence the reliability is  $\mathcal{R}(k) = \sum_{\mathbf{n}, \mathbf{n}'} |C(\mathbf{n})|^2 |C(\mathbf{n}')|^2 \cos[\gamma_{\xi_0,1}(\tau) \mathbf{1}^T (\mathbf{n} - \mathbf{n}')] \exp[-(\mathbf{n} - \mathbf{n}')^T \mathbf{\Sigma} (\mathbf{n} - \mathbf{n}')/(2N)]$ , where the off-diagonal elements of  $\mathbf{\Sigma}$  are  $\mathbf{\Sigma}_{m \neq l} = \text{Cov}(\mathcal{D}_l, \mathcal{D}_m)/(N\Delta) + \text{Cov}(\mathcal{G}_l, \mathcal{G}_m)/(Ng)$ , which represents the correlations between  $m, l$ -th processes, here  $\text{Cov}(\cdot_l, \cdot_m) := \langle (\cdot_l - \langle \cdot_l \rangle)(\cdot_m - \langle \cdot_m \rangle) \rangle$ . Since procedure (1) involves repeated operations on the same system, the correlations become maximal, i.e.,  $\Sigma_{l \neq m} \rightarrow \Sigma_{l=m} = \Gamma_{\xi_0}(\tau)$ . Therefore, such correlations could significantly reduce the reliability of memory-based devices, whereas enhancing the independence across cycles ( $\Sigma_{l \neq m} \rightarrow 0$ ), straightforwardly suppresses the loss. The upper bound on reliability is Eq.(A2), and it is noteworthy that it can factor into the product of state fidelity (reliability)  $\mathcal{R}(1) = \mathcal{F}(\tau)$  of single cycle, reads

$$\begin{aligned} \mathcal{F}(\tau) &= \sum_{n, n'} |C_n|^2 |C_{n'}|^2 \cos[(n - n')\gamma_{\xi_0,1}(\tau)] \times \quad (6) \\ &\quad \times \exp\{-(n - n')^2 \Gamma_{\xi_0}(\tau)/(2N)\}, \end{aligned}$$

where  $\Gamma_{\xi_0}(\tau) = (\delta\Delta/\Delta)^2 \gamma_{\xi_0,1}^2(\tau) + (\delta g/g)^2 \mu_{\xi_0,1}^2(\tau)$ .

Therefore, we can subsequently focus on  $\mathcal{F}(\tau)$  for simplicity.

It is noteworthy that when detuning is ignored, one can obtain  $\mathcal{F} = 1$ , hence disordered coupling strength has not impact on storage performance, recovering the conclusion of [22]. It follows from (5) that the detrimental effect of disordered coupling on quantum memory arises from its correlation with detuning (i.e.,  $\mu_{\xi_0,1} \varepsilon_g$ ), and is therefore triggered by the presence of detuning. This reveals that some imperfections act primarily through their correlations, not individually.

*Toward reliable global detuning measurement.*— It can be proved that despite an unavoidable  $\Delta$  [13, 20, 21], the oscillatory term in Eq.(6) (leading term in Eq.(5)) can be eliminated via applying a compensation  $U_{\text{com}} = \exp(-i\gamma_{\xi_0,1}(\tau) \hat{a}^\dagger a)$  to  $|\phi_{\text{out}}\rangle$ . When  $\Delta$  is unknown, a universal method is to perform quantum tomography [8, 13, 21] on a detection state  $|\phi_{\text{in}}^{(\text{de})}\rangle$  that undergoes SIRO process (prior to function as a quantum memory), since  $\Delta$  induces a rotation of Wigner function of  $\forall |\phi_{\text{in}}\rangle$  around the origin by a mean phase

$$\bar{\varphi} = \gamma_{\xi_0,1}(\tau) = \Delta(\tau_s + \kappa_\theta \tau_d), \quad (7)$$

where we define the adiabatic pulse factor  $\kappa_\theta := \int_0^{\tau_d} dt/(\tau_d) \sin^2 \tilde{\theta}_{g_0}(t/\tau_d)$  with  $\tilde{\theta}_{g_0}(t/\tau_d) := \theta_{g_0}(t)$ , determined solely by driving waveform, e.g.,  $\kappa_\theta \simeq 3.2$  shown in Fig. 1.

We emphasize that achieving precise measurements and more reliable storage necessitate accounting for the Berry's phase (especially the term  $\kappa_\theta$ ) in current experiments [13, 21, 36]. It can be shown (please see Sec.III in SM [30]) that the omission of the Berry's phase (the term  $\kappa_\theta$ ) leads to a residual detuning

$$\delta^{(\text{de})} = \Delta^{(\text{de})} - \Delta = \alpha_\theta \tau_d^{(\text{de})} \Delta / (\tau_s^{(\text{de})} + \tau_d^{(\text{de})}/2), \quad (8)$$

which persists even after compensation or field frequency adjustment, where  $\Delta^{(\text{de})}$  denotes the measured detuning, and  $\alpha_\theta := \kappa_\theta - 1/2$ . This renders a phase error  $\delta^{(\text{de})} \tau_s$  in a real storage process.

Although Eq.(8) implies the condition  $\tau_s^{(\text{de})}/\tau_d^{(\text{de})} \gg 1$  is sufficient to suppress the residue detuning  $\delta^{(\text{de})}$ , the reliability loss induced by the omission is significantly amplified by large storage time  $\tau_s$ . To demonstrate the phenomenon, an example of storing a coherent state  $|\phi_{\text{in}}\rangle = |\alpha\rangle$  is investigated. Let  $\delta\Delta = \delta g = 0$  for simplicity. After single SIRO cycle, the fidelity is  $\mathcal{F} \simeq \exp[-2|\alpha|^2(1 - \cos(\delta^{(\text{de})} \tau_s))]$  based on Eq.(6). Fig. 2 shows the fidelity  $\mathcal{F}$  drops significantly with increasing  $|\alpha|$  and  $\tau_s$ . Moreover, by expanding Eq.(6) to leading term, we obtain  $\tau_s^{(\text{de})}/\tau_d^{(\text{de})} \gg \Delta \tau_s (\Delta n^2)^{1/2}$  to ensure high fidelity. It shows achieving a universal quantum memory with long storage time requires more constraints on  $\tau_s^{(\text{de})}$  and  $\langle \Delta n^2 \rangle := \langle (\hat{a}^\dagger \hat{a})^2 \rangle - \langle \hat{a}^\dagger \hat{a} \rangle^2$  of stored states. Therefore, Eq.(7) provides a more reliable measurement

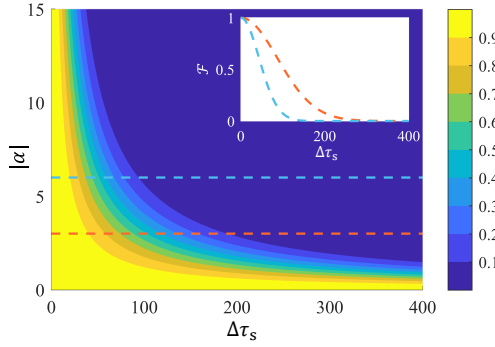


FIG. 2. fidelity  $\mathcal{F}$  versus  $|\alpha|$  and storage time  $\tau_s$  with  $\tau_s^{(\text{de})}/\tau_d^{(\text{de})} = 1000$  and  $\alpha_\theta = 2.7$ . Inset represents the fidelity  $\mathcal{F}$  versus  $\tau_s$  for  $|\alpha| = 3$  (orange) and  $|\alpha| = 6$  (blue), which corresponds to the vertical dashed line.

relation, directly supporting long-time and high-capacity storage.

*Effects of disorders.*— The above discussion enables us to concentrate on the effect of broadening  $\delta\Delta$  and disordered coupling  $\delta g$ , with  $\cos[(n - n')\gamma_{\xi_0,1}(\tau)] \simeq 1$ . Combining physical realizability, we focus on stored states that satisfy two conditions (see *Appendix B*). Here we find that in the regime of  $\langle \Delta n^2 \rangle \gg 1$ , the fidelity can be approximated as a universal form (see Sec. IV in SM [30] for detailed discussion and proof)

$$\mathcal{F}(\tau) \simeq \sum_m \frac{c_m}{m!} [-\Gamma_{\xi_0}(\tau)\langle \Delta n^2 \rangle/N]^m, \quad (9)$$

where  $c_m$  is determined by the stored state and index  $m$ . It is noteworthy that, physically these conditions demand the state is well-localized around  $\langle n \rangle$  to ensure finite all-order photon number moments  $\sum_n |C_n|^2 n^j$ , and the distribution of  $Z_{n,\langle \Delta n^2 \rangle} := (n - \langle n \rangle)/\langle \Delta n^2 \rangle$  tends to stabilize with  $\langle \Delta n^2 \rangle \gg 1$ . These features are manifest in some significant states in quantum communication and quantum computation, such as cat, squeezed states [13, 37, 38].

Notably, it follows from Eq.(9) that  $\Gamma_{\xi_0}(\tau)$  (i.e., detuning and disordered coupling) solely constraint  $\langle \Delta n^2 \rangle$  of stored state with a universal inverse proportionality for fixed fidelity. Here, cat state and uniform superposition state are used as examples (see Sec.V in SM [30] for details). Fig. 3 (a) shows the exact form of fidelity for cat state versus  $\langle \Delta n^2 \rangle$  and  $\Gamma_{\xi_0}(\tau)/N$ , it can be observed that the constant-fidelity contours (solid lines) converge towards the hyperbolic dashed line which represents the inverse proportionality  $\Gamma_{\xi_0}(\tau)/N \propto 1/\langle \Delta n^2 \rangle$ . Moreover, Fig. 3 (b) shows the behaviors of the fidelity of these states as a function of  $\Gamma_{\xi_0}(\tau)\langle \Delta n^2 \rangle/N$ , the square and circle denote the approximate form consistent with Eq.(9). It is observed from inset that both forms exhibit power-law tail behavior, scaling as  $(\Gamma_{\xi_0}(\tau)\langle \Delta n^2 \rangle/N)^{-1/2}$ . Moreover, it can be proven that

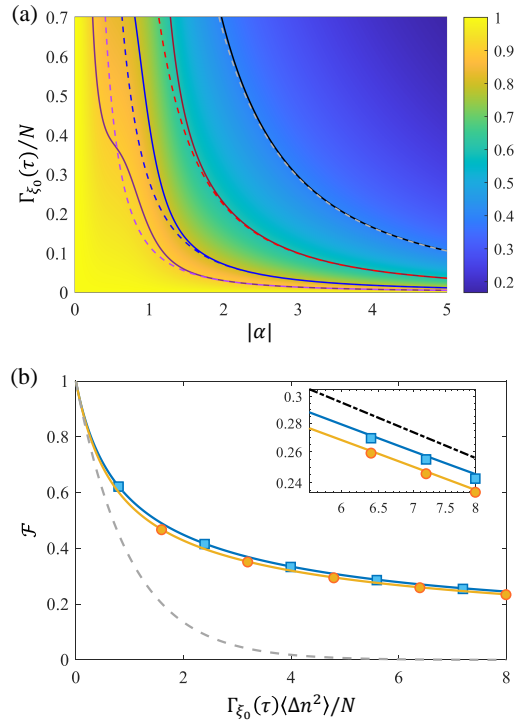


FIG. 3. (a) fidelity  $\mathcal{F}$  versus  $\Gamma_{\xi_0}(\tau)/N$  and  $|\alpha|$ , when storing cat state  $\mathcal{N}_0(|\alpha\rangle + \exp(\eta + i\theta)|-\alpha\rangle)$ ,  $\eta, \theta \in \mathbb{R}$ , here we set  $\eta = 1, \theta = \pi$ . The curves represent contours of  $\mathcal{F} = 0.9, 0.8, 0.6, 0.4$  from left to right, with solid lines for the exact form, and dashed lines for the approximate form when  $\langle \Delta n^2 \rangle \gg 1$  (here  $\langle \Delta n^2 \rangle \simeq |\alpha|^2$ ), following a relation  $\Gamma_{\xi_0}(\tau)/N \propto 1/|\alpha|^2$ . (b)  $\mathcal{F}$  versus  $\Gamma_{\xi_0}\langle \Delta n^2 \rangle/N$ . The blue and orange solid lines represent storing the cat state ( $\eta = 0, \theta = 0$ ) and the uniform superposition state, respectively, with  $\langle \Delta n^2 \rangle = 10$ . Squares and circles represent the approximate form. The dashed line is lower bound for arbitrary state fidelity, and the inset shows scaling as  $(\Gamma_{\xi_0}(\tau)\langle \Delta n^2 \rangle/N)^{-1/2}$ . Please see Sec... in SM for detailed derivation of such forms for these states.

(see Sec.VI in SM [30]) the fidelity satisfies

$$\mathcal{F}(\tau) \geq \exp(-\Gamma_{\xi_0}(\tau)\langle \Delta n^2 \rangle/N), \quad (10)$$

for any stored state and  $\langle \Delta n^2 \rangle$ , where the lower bound (gray dashed line) exhibits universal exponential decay.

*Trade-off in a reliable universal quantum memory.*— Drawing from the above analysis and Eq.(10), a general trade-off for storage capacity, storage and driving time of a quantum memory can be presented as

$$1 - \mathcal{F}_0 \simeq (\delta\Delta^2\tau_s^2 + \Delta^2\delta g^2\zeta_\theta^2\tau_d^2/g^2)(\exp \mathcal{C} - 1)^2/(4N), \quad (11)$$

in highly reliable region. Notably, the information-storage capacity is found to be directly related to the photon number fluctuation, i.e.,  $\mathcal{C} \simeq \ln\{(4\langle \Delta n^2 \rangle_{\text{max}})^{1/2} + 1\}$  (please see Sec.VII in SM [30] for details), where  $\langle \Delta n^2 \rangle_{\text{max}}$  denotes the maximum photon number fluctuation allowed for stored states,  $\mathcal{F}_0$  is the corresponding fidelity, while also serving as the lower bound for all stored

states supported by this capacity. Here, we introduce the adiabatic pulse factor  $\zeta_\theta := \int_0^{\tau_d} d(t/\tau_d) \sin^2(2\tilde{\theta}_{g_0}(t/\tau_d))$ , following the definition of  $\kappa_\theta$ , such as  $\zeta_\theta \simeq 2.7$  shown in Fig. 1.

It is observed that the broadening  $\delta\Delta$  primarily constrains the storage time  $\tau_s$ , but the disordered coupling and global detuning  $\Delta$  solely limits the driving time  $\tau_d$ . Moreover, there exists a constraint  $\tau_d, 1/|\Delta| \gg \sqrt{n_{\max}/(Ng^2)}$  with  $\sum_{n_{\max}}^\infty |C_n|^2 \ll 1$  based on adiabatic condition (please see Sec.II in SM [30] for derivation). Therefore, these results provide precise targets for optimizing the relevant quantities.

To further illustrate the trade-off, the recently demonstrated cold-atom platform for quantum memory [6, 39–42] is considered. As an order-of-magnitude estimate, the atomic cloud width is  $d \sim 1$  cm [42], the signal beam waist is  $w_0 \sim 100\mu\text{m}$  and the typical atomic density is  $n \sim 10^{11}\text{cm}^{-3}$  [41], leading to the effective atom number of  $N \sim nw_0^2d \sim 10^7$ . For a broadening  $\delta\Delta \sim 1\text{MHz}$  in EIT-memory [43], achieving  $\mathcal{F}_0 = 0.9$  requires time and capacity to satisfy the trade-off  $\tau_s \exp \mathcal{C} \simeq 1\text{ms}$ , which likewise requires all stored states to obey  $\langle \Delta n^2 \rangle^{1/2} \tau_s \lesssim 1\text{ms}$ .

It is noteworthy that many protocols deliberately introduce detuning or disordered coupling to enhance storage efficiency [13], to realize geometric quantum memory [20], or to effectively suppress decoherence by exploiting nuclear spin waves [23, 24]. In addition, AC-stark shifts from strong control field can reach MHz scale [17]. These situations underscore the need to carefully address the correlated effects of detuning and disordered coupling. As an illustration, with average coupling strength  $g \sim 0.1\text{MHz}$  and  $\delta g/g \sim 0.1$ , there exists a trade-off  $\Delta \tau_d \exp \mathcal{C} \simeq 10^5$  (equivalently  $\Delta \tau_d \langle \Delta n^2 \rangle^{1/2} \lesssim 10^5$  for stored states) to maintain  $\mathcal{F}_0 = 0.9$ , and the adiabatic condition demands  $|\Delta|, 1/\tau_d \ll 10^{2.5}/n_{\max}^{1/2} \text{MHz} \sim 10^{2.5}/\langle \Delta n^2 \rangle^{1/2} \text{MHz}$ . Notably, recent proposals for fiber-coupled quantum memory [41, 44–47], which guide the retrieval light efficiently, could reduce the effective atom number to  $N \sim 10^3 - 10^4$  [44, 45, 47], thereby making the trade-off become more stringent.

*Conclusion.*— We develop a comprehensive model to investigate the impact of inevitable disordered coupling and detuning on the quantum information content stored in a universal EIT-based quantum memory. These imperfections induce a random Berry’s phase on a stored state and impose a constraint of universal form on the photon number fluctuation  $\langle \Delta n^2 \rangle$  for typical states that possess characteristics relevant to practical applications. Consequently, a general and intrinsic trade-off among storage capacity, storage and driving time is further established for a highly reliable universal quantum memory which applies to arbitrary states. In particular, the results indicate the broadening primarily limits the storage time, while disordered coupling only restricts the driving time, which provide precise optimization targets for specific pa-

rameters.

Notably, our results suggest that certain imperfections like disordered coupling degrade the memory only through their correlation with other factors (e.g., detuning), rather than individually. This implies that correlation effects of some factors can lead to qualitatively different behavior from isolated analyses. These findings are directly relevant to protocols that involve disordered coupling [23, 25] and introduce detuning [13, 20]. Moreover, they can be further applicable to geometric and holographic quantum computation [48, 49].

In addition, the reliability of typical processes in memory-based devices [33–35] is examined, revealing that enhancing the independence among different storage processes can suppress reliability-loss of devices. Separately, it is pointed that global detuning measurements must incorporate the Berry’s phase, otherwise, the induced reliability loss of memory grows significantly with capacity and storage time, hence a precise measurement relation is provided.

*Acknowledgment.*— This work was supported by the Science Challenge Project (Grant No. TZ2025017), the National Natural Science Foundation of China (NSFC) (Grant No. 12088101), the NSAF (Grant No. U2330401).

\* ymdu@gscap.ac.cn

† suncp@gscap.ac.cn

- [1] N. Gisin and R. Thew, *Nat. photonics* **1**, 165 (2007).
- [2] V. Scarani, H. Bechmann-Pasquinucci, N. J. Cerf, M. Dušek, N. Lütkenhaus, and M. Peev, *Rev. Mod. Phys.* **81**, 1301 (2009).
- [3] A. I. Lvovsky, B. C. Sanders, and W. Tittel, *Nat. photonics* **3**, 706 (2009).
- [4] N. D. Mermin, *Quantum computer science: an introduction* (Cambridge University Press, 2007).
- [5] P. W. Shor, *Phys. Rev. A* **52**, R2493 (1995).
- [6] R. Zhao, Y. Dudin, S. Jenkins, C. Campbell, D. Matsukevich, T. Kennedy, and A. Kuzmich, *Nat. Phys.* **5**, 100 (2009).
- [7] Z.-L. Zhang and L.-P. Yang, *Phys. Rev. A* **107**, 063704 (2023).
- [8] Y. Hashimoto, T. Toyama, J.-i. Yoshikawa, K. Makino, F. Okamoto, R. Sakakibara, S. Takeda, P. van Loock, and A. Furusawa, *Phys. Rev. Lett.* **123**, 113603 (2019).
- [9] C. P. Sun, Y. Li, and X. F. Liu, *Phys. Rev. Lett.* **91**, 147903 (2003).
- [10] M. Lukin, S. Yelin, and M. Fleischhauer, *Phys. Rev. Lett.* **84**, 4232 (2000).
- [11] M. Fleischhauer and M. D. Lukin, *Phys. Rev. A* **65**, 022314 (2002).
- [12] C. P. Sun, S. Yi, and L. You, *Phys. Rev. A* **67**, 063815 (2003).
- [13] J. Appel, E. Figueroa, D. Korystov, M. Lobino, and A. I. Lvovsky, *Phys. Rev. Lett.* **100**, 093602 (2008).
- [14] F. Kimiae Asadi, J. Kumar, J. Ji, K. Heshami, and C. Simon, *Phys. Rev. Lett.* **135**, 070802 (2025).

[15] Y.-C. Wei, B.-H. Wu, Y.-F. Hsiao, P.-J. Tsai, and Y.-C. Chen, Phys. Rev. A **102**, 063720 (2020).

[16] A. D Greentree, R. G. Beausoleil, L. C. L. Hollenberg, W. J. Munro, K. Nemoto, S. Prawer, and T. P. Spiller, New. J. Phys **11**, 093005 (2009).

[17] Y.-F. Hsiao, P.-J. Tsai, H.-S. Chen, S.-X. Lin, C.-C. Hung, C.-H. Lee, Y.-H. Chen, Y.-F. Chen, I. A. Yu, and Y.-C. Chen, Phys. Rev. Lett. **120**, 183602 (2018).

[18] L. Esguerra, L. Meßner, E. Robertson, N. V. Ewald, M. Gündoğan, and J. Wolters, Phys. Rev. A **107**, 042607 (2023).

[19] U. Schnorrberger, J. D. Thompson, S. Trotzky, R. Puigatch, N. Davidson, S. Kuhr, and I. Bloch, Phys. Rev. Lett. **103**, 033003 (2009).

[20] Y. Li, P. Zhang, P. Zanardi, and C. P. Sun, Phys. Rev. A **70**, 032330 (2004).

[21] M. Lobino, C. Kupchak, E. Figueroa, and A. I. Lvovsky, Phys. Rev. Lett. **102**, 203601 (2009).

[22] X.-J. Liu, Z.-X. Liu, X. Liu, and M.-L. Ge, Phys. Rev. A **73**, 013825 (2006).

[23] Z. Song, P. Zhang, T. Shi, and C.-P. Sun, Phys. Rev. B **71**, 205314 (2005).

[24] Z. Kurucz, M. W. Sørensen, J. M. Taylor, M. D. Lukin, and M. Fleischhauer, Phys. Rev. Lett. **103**, 010502 (2009).

[25] I. Diniz, S. Portolan, R. Ferreira, J. M. Gérard, P. Bertet, and A. Auffèves, Phys. Rev. A **84**, 063810 (2011).

[26] L. X. Cui, Y.-M. Du, and C. P. Sun, Phys. Rev. Lett. **131**, 160203 (2023).

[27] L.-X. Cui, Y.-M. Du, and C.-P. Sun, J. Reliab. Sci. Eng. **1**, 015004 (2025).

[28] Y.-Q. Liu, Y.-M. Du, and X. Wang, Phys. Rev. A **112**, 022207 (2025).

[29] Y. Li, Y.-M. Du, W. Ding, Z. Fei, L. Fu, and X. Wang, Phys. Rev. A **112**, 032220 (2025).

[30] Please see Supplemental Material for details.

[31] A. S. Holevo, *Quantum systems, channels, information: a mathematical introduction* (Walter de Gruyter GmbH & Co KG, 2019).

[32] M. A. Nielsen and I. L. Chuang, *Quantum computation and quantum information* (Cambridge university press, 2010).

[33] P. Kok, W. J. Munro, K. Nemoto, T. C. Ralph, J. P. Dowling, and G. J. Milburn, Rev. Mod. Phys. **79**, 135 (2007).

[34] S. Pirandola, Commun Phys **2**, 51 (2019).

[35] K. Azuma, S. E. Economou, D. Elkouss, P. Hilaire, L. Jiang, H.-K. Lo, and I. Tzitrin, Rev. Mod. Phys. **95**, 045006 (2023).

[36] Y.-H. Chen, M.-J. Lee, I.-C. Wang, and I. A. Yu, Phys. Rev. A **88**, 023805 (2013).

[37] B. Vlastakis, G. Kirchmair, Z. Leghtas, S. E. Nigg, L. Frunzio, S. M. Girvin, M. Mirrahimi, M. H. Devoret, and R. J. Schoelkopf, Science **342**, 607 (2013).

[38] S. Konno, W. Asavanant, F. Hanamura, H. Nagayoshi, K. Fukui, A. Sakaguchi, R. Ide, F. China, M. Yabuno, S. Miki, H. Terai, K. Takase, M. Endo, P. Marek, R. Filip, P. van Loock, and A. Furusawa, Science **383**, 289 (2024).

[39] J. Wang, L. Dong, X. Wang, Z. Zhou, J. Huang, Y. Zuo, G. A. Siviloglou, and J. F. Chen, Phys. Rev. Res. **6**, L042002 (2024).

[40] D.-S. Ding, W. Zhang, Z.-Y. Zhou, S. Shi, J.-s. Pan, G.-Y. Xiang, X.-S. Wang, Y.-K. Jiang, B.-S. Shi, and G.-C. Guo, Phys. Rev. A **90**, 042301 (2014).

[41] C. Sayrin, C. Clausen, B. Albrecht, P. Schneeweiss, and A. Rauschenbeutel, Optica **2**, 353 (2015).

[42] Y. Wang, J. Li, S. Zhang, K. Su, Y. Zhou, K. Liao, S. Du, H. Yan, and S.-L. Zhu, Nat. Photonics **13**, 346 (2019).

[43] G. Buser, R. Mottola, B. Cotting, J. Wolters, and P. Treutlein, PRX Quantum **3**, 020349 (2022).

[44] B. Gouraud, D. Maxein, A. Nicolas, O. Morin, and J. Laurat, Phys. Rev. Lett. **114**, 180503 (2015).

[45] W. S. Leong, M. Xin, C. Huang, Z. Chen, and S.-Y. Lan, Phys. Rev. Res. **2**, 033320 (2020).

[46] F. Blatt, L. S. Simeonov, T. Halfmann, and T. Peters, Phys. Rev. A **94**, 043833 (2016).

[47] M. Xin, W. S. Leong, Z. Chen, and S.-Y. Lan, Phys. Rev. Lett. **122**, 163901 (2019).

[48] J. Zhang, T. H. Kyaw, S. Filipp, L.-C. Kwek, E. Sjöqvist, and D. Tong, Physics Reports **1027**, 1 (2023), geometric and holonomic quantum computation.

[49] L.-A. Wu, P. Zanardi, and D. A. Lidar, Phys. Rev. Lett. **95**, 130501 (2005).

[50] R. B. Griffiths, J. Stat. Phys. **36**, 219 (1984).

[51] R. B. Griffiths, *Consistent quantum theory* (Cambridge University Press, 2003).

[52] D. Bertsekas and J. N. Tsitsiklis, *Introduction to probability*, Vol. 1 (Athena Scientific, 2008).

## End Matter

*Appendix A: specific form of reliability.*— It follows from Eq.(5) the output state approximately depends solely on collective detuning  $\mathcal{D} := \sum_j \Delta_j$  and collective CS  $\mathcal{G} := \sum_j g_j$ , we therefore denotes the single SIRO process associated with a set of specific  $\xi$  as  $|\phi_{\text{out},\xi}\rangle = U_{\Xi}(\tau)|\phi_{\text{in}}\rangle$ , where the subscript  $\Xi := \{\mathcal{D}, \mathcal{G}\}$ . Moreover, based on the central-limit theorem,  $\mathcal{D} \sim \mathcal{N}(N\Delta, N\delta\Delta^2)$  and  $\mathcal{G} \sim \mathcal{N}(Ng, N\delta g^2)$ . Process (1): Fig. A1 (a) illustrates the key procedure of a synchronizer in a quantum channel. The synchronizer is based on quantum memory that performs a SIRO process on a state in the channel to introduce a time delay, thereby synchronizing it with parallel states of other channels in subsequent operations [3, 33]. Here, the memory is assumed to per-

form SIRO on a sequence of  $k$  states  $\{|\phi_{\text{in}}^{(1)}\rangle, \dots, |\phi_{\text{in}}^{(k)}\rangle\}$ , with  $|\phi_{\text{in}}^{(j)}\rangle = \sum_n C_n^{(j)}|n\rangle_L$ . Based on the framework of quantum reliability [26–29], the reliable trajectory for a specific set of  $\xi$  is  $|\phi_{\text{in}}^{(1)}\rangle - U_{\mathcal{G}}(\tau_1) \rightarrow \text{reliable} \dashrightarrow |\phi_{\text{in}}^{(2)}\rangle - U_{\mathcal{G}}(\tau_2) \rightarrow \text{reliable} \dashrightarrow \dots$ . Where  $\tau_j$  represents the synchronization time for the  $j$ -th state, and the dashed lines indicate the intermediate process of retrieving out one state and storing the next. Since we focus on the reliability of SIRO processes at the solid arrow, the above trajectory is equivalent to  $|\Phi_{\text{in}}\rangle - \mathbf{U}_{\Xi} \rightarrow \text{reliable}$ , with  $|\Phi_{\text{in}}\rangle := \prod_j^k \otimes |\phi_{\text{in}}^{(j)}\rangle$  and  $\mathbf{U}_{\Xi} = \prod_j^k \otimes U_{\mathcal{G}}(\tau_j)$  [50, 51]. In the letter, we consider  $\tau_j = \tau, \forall j$  to simplify the subsequent discussion. The reliability is written as a compact

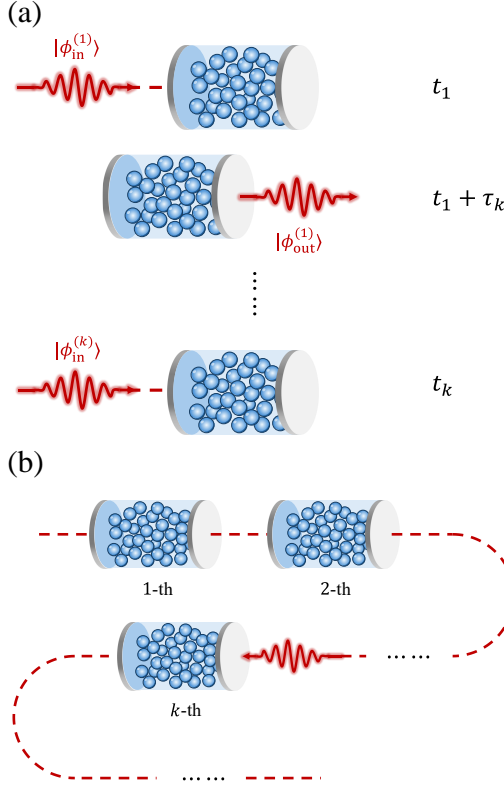


FIG. A1. The key procedure of typical memory-based devices, i.e., the synchronizer and repeater chains: (a) the memory performs SIRO on a sequence of  $k$  states, (b) a state undergoes  $k$  memory-based repeaters.

form

$$\begin{aligned} \mathcal{R}_S(k) &= \langle \text{Tr}[\mathbf{E} \mathbf{U}_\Xi | \Phi_{\text{in}} \rangle \langle \Phi_{\text{in}} | \mathbf{U}_\Xi^\dagger \mathbf{E}^\dagger] \rangle_\Xi \\ &= \sum_{\mathbf{n}, \mathbf{n}'} |C(\mathbf{n})|^2 |C(\mathbf{n}')|^2 \cos[\gamma_{\xi_0, 1}(\tau) \mathbf{1}^T (\mathbf{n} - \mathbf{n}')] \times \\ &\quad \times \exp[-(\mathbf{n} - \mathbf{n}')^T \mathbf{1} \mathbf{1}^T (\mathbf{n} - \mathbf{n}') \Gamma_{\xi_0}(\tau) / (2N)], \end{aligned} \quad (\text{A1})$$

where  $\mathbf{n} = (n_1, \dots, n_k)^T \in \mathbb{N}^k$ ,  $\mathbf{1} = (1, \dots, 1)^T$ ,  $C(\mathbf{n}) = \prod_j^k C_{n_j}^{(j)}$ , and  $\mathbf{E} = |\Phi_{\text{in}}\rangle \langle \Phi_{\text{in}}|$ . Here,  $\langle \cdot \rangle_\Xi$  represents averaging over random variable  $\Xi$ , which is equivalent to averaging over all random  $\Delta_j$  and  $g_j$  [52].

Process (2): Fig. A1 (b) shows the process of repeater chains in quantum network [1, 34, 35], where an arbitrary optical state  $|\phi_{\text{in}}\rangle$  undergoes  $k$  repeaters implemented by such memories. It follows from that the reliable trajectory is  $|\phi_{\text{in}}\rangle - U_{\Xi_1}(\tau_1) \rightarrow \text{reliable} \dots - U_{\Xi_k}(\tau_k) \rightarrow \text{reliable}$ ,

where the subscript  $\Xi_j$  corresponds to  $j$ -th quantum memory. Here the collective CS and detuning in different quantum memories are treated as independent, since there is no direct interaction between each quantum memories. It is likewise considered that  $\tau_j = \tau, \forall j$ , the reliability is written as

$$\begin{aligned} \mathcal{R}_R(k) &= \langle \text{Tr}[\prod_{j=1}^k E U_{\Xi_j}(\tau) |\phi_{\text{in}}\rangle \langle \phi_{\text{in}}| \prod_{j=1}^k U_{\Xi_j}^\dagger(\tau) E^\dagger] \rangle_{\Xi_1, \dots, \Xi_k} \\ &= \sum_{\mathbf{n}, \mathbf{n}'} |C(\mathbf{n})|^2 |C(\mathbf{n}')|^2 \cos[\gamma_{g_0, 1}(\tau) \mathbf{1}^T (\mathbf{n} - \mathbf{n}')] \times \\ &\quad \times \exp[-(\mathbf{n} - \mathbf{n}')^T (\mathbf{n} - \mathbf{n}') \Gamma_{\xi_0}(\tau) / (2N)], \end{aligned} \quad (\text{A2})$$

where  $\langle \cdot \rangle_{\Xi_1, \dots, \Xi_k}$  denotes averaging over all  $\Xi_1, \dots, \Xi_k$ , and  $C(\mathbf{n})$  is replaced with  $\prod_j^k C_{n_j}$ . It is observed that, in contrast to (A1), the reliability (A2) can factorize into the product of identical SIRO process, i.e.,  $\mathcal{R}_R(k) = [\mathcal{R}_R(1)]^k$ .

*Appendix B: condition of approximation.*— Regarding the stored state  $|\phi_{\text{in}}\rangle = \sum_n C_n |n\rangle_L$  with average photon number  $\langle n \rangle$  and fluctuation  $\langle \Delta n^2 \rangle$ , We first

condition (1):  $|C_n|^2$  follows light-tailed distribution, where

$$\sum_{|n - \langle n \rangle| \geq u} |C_n|^2 \leq C \exp(-\chi u^\delta), \quad \exists C, \chi, \delta > 0, \quad \forall u > 0. \quad (\text{B1})$$

In other words, the decay behavior of  $|C_n|^2$  as it deviates from  $\langle n \rangle$  is analogous to exponential type decay or even faster.

condition (2): The distribution of state exhibit weak convergence in response to  $\langle \Delta n \rangle$ . The condition is described as follows:

We define the normalized random variable

$$Z_{n, \langle \Delta n^2 \rangle} = (n - \langle n \rangle) / \langle \Delta n^2 \rangle^{1/2},$$

with mean value  $\langle Z_{n, \langle \Delta n^2 \rangle} \rangle = \sum_n |C_n|^2 Z_{n, \langle \Delta n^2 \rangle} = 0$ , and variance  $\langle \Delta Z_{n, \langle \Delta n^2 \rangle} \rangle = 1$ , its distribution is

$$F_{\langle \Delta n^2 \rangle}(y) = \sum_{y \geq Z_{n, \langle \Delta n^2 \rangle}} |C_n|^2. \quad (\text{B2})$$

Then  $\exists F_Z(y)$ ,

$$\lim_{\langle \Delta n^2 \rangle \rightarrow \infty} F_{\langle \Delta n^2 \rangle}(y) = F_Z(y). \quad (\text{B3})$$